Title	Correlated Sources Transmission in Orthogonal Multiple Access Relay Channel: Theoretical Analysis and Performance Evaluation
Author(s)	Zhou, Xiaobo; Lu, Pen-Shun; Anwar, Khoirul; Matsumoto, Tad
Citation	IEEE Transaction on Wireless Communications, 13(3): 1424-1435
Issue Date	2014-01-21
Type	Journal Article
Text version	author
URL	http://hdl.handle.net/10119/11565
Rights	This is the author's version of the work. Copyright (C) 2014 IEEE. IEEE Transaction on Wireless Communications, 13(3), 2014, 1424-1435. Personal use of this material is permitted. Permission from IEEE must be obtained for all other uses, in any current or future media, including reprinting/republishing this material for advertising or promotional purposes, creating new collective works, for resale or redistribution to servers or lists, or reuse of any copyrighted component of this work in other works.
Description	

Correlated Sources Transmission in Orthogonal Multiple Access Relay Channel: Theoretical Analysis and Performance Evaluation

Xiaobo Zhou, *Member, IEEE,* Pen-Shun Lu, *Student Member, IEEE,* Khoirul Anwar, *Member, IEEE,*
and Tad Matsumoto, *Fellow, IEEE*

Abstract—In this paper, we consider the problem of transmitting two correlated binary sources over orthogonal multiple access relay channel (MARC), where two sources are communicating with a common destination with the assistance of a single relay. We assume decode-and-forward relaying strategy, and bit-wise exclusive or (XOR) network coding is performed at the relay node. First, a joint source-channel-network (JSCN) decoding technique is proposed to fully exploit the correlation between the sources, as well as the benefit of network coding. Then the achievable compression rate region of this system is derived based on the theorem for source coding with side information. It is found that the region is a 3-dimensional space surrounded by a polyhedron. Furthermore, the performance limit in Additive White Gaussian Noise (AWGN) channels and the outage probability in block Rayleigh fading channels are derived based on the achievable compression rate region. It is shown that the outage probability can be expressed by a set of triple integrals over the achievable compression rate region. The impact of source correlation on the performance of the system is investigated through asymptotic tendency analysis. The effectiveness of the proposed JSCN decoding technique and the accuracy of the theoretical analysis have been verified through a series of computer simulations, assuming practical channel codes. It is also shown that, as long as the source-relay links are perfect, the *2nd* order diversity is always achieved with our proposed technique regardless of the strength of the source correlation.

Index Terms—Multiple Access Relay Channel, decode-and-forward, correlated sources, joint source-channel-network coding, source coding with side information theorem, outage probability

I. INTRODUCTION

WIRELESS sensor networks (WSNs) [1] made up of a great number of densely deployed low-energy consuming wireless nodes (e.g. micro cameras and small relays) have attracted a lot of attention recently, and its potential applications cover a vast area of human activities, such as wireless video surveillance, environmental monitoring, health care system, and many other possible applications [2]. There

X. Zhou and K. Anwar are with School of Information Science, Japan Advanced Institute of Science and Technology, 1-1 Asahidai, Nomi, Ishikawa 923-1292, Japan (e-mail:{xiaobo, anwar-k}@jaist.ac.jp).

P.-S. Lu and T. Matsumoto are with School of Information Science, Japan Advanced Institute of Science and Technology, 1-1 Asahidai, Nomi, Ishikawa 923-1292, Japan, and with Centre for Wireless Communications, University of Oulu, P.O. Box 4500, 90014 University of Oulu, Finland (e-mail: {penshun, tadashi.matsumoto}@ee.oulu.fi).

are several inherent properties within WSNs that make the problem interesting: (1) the correlation exists between the data collected at the wireless nodes, (2) the wireless nodes can exchange information to increase their efficiency or flexibility through cooperation, (3) the wireless nodes have energy consumption limit, and hence their computational capability is also limited. Therefore the signaling complexity as well as transmitting power have to be as low as possible. Hence, the problem of optimal code design for WSNs that makes efficient use of the advantage of correlation knowledge among sources as well as achieving spatial diversity through node cooperation falls into the category of network coding for correlated sources [3], [4].

It has been shown in [5] that the problem of transmitting correlated sources over the cooperative networks involves the issues of network coding [6] and distributed source coding [7]. In the initial stage, network coding and distributed source coding were performed separately [5]. Network coding provides cooperative diversity for fading mitigation while distributed source coding exploits the correlation among sources for efficient source compression. However, it is well known that in practical networks such as WSNs with limited complexity, separate design of source, channel and network coding may not be optimal [8].

Recently, joint source-channel-network (JSCN) coding has emerged as a promising technique for correlated sources transmission over the cooperative networks. This problem was originally investigated in [9], where a general network of discrete memoryless channels (DMCs) with multiple relay nodes and a single sink node is considered. Later, multicasting of correlated sources over a network of noiseless channels were considered in [3], where error exponents are provided. Reference [4] provides theorems with their proofs that can be used as a theoretical basis for solving the problem of network information flow with correlated sources. Following the theoretical investigations described above, some practical JSCN coding schemes have also been proposed [10]–[13]. A JSCN coding scheme for bidirectional wireless relays based on fountain code is proposed in [12], and JSCN coding schemes for multicasting are presented in [5], [8], [11]. A similar work for combining JSCN coding and Turbo equalization in Multiple Access Relay Channel (MARC) is shown in [10], where the relay node multiplexes and re-encodes the data sequences transmitted from the two source nodes. However, if bit-wise exclusive or (XOR) network coding [14] is employed at the

Fig. 2. The block diagram of the proposed system. ENC_1, ENC_2 and ENC_r are channel codes for S_1, S_2 and S_r, respectively.

relay node, efficient JSCN coding scheme design, theoretical performance limit calculation, and rate region analysis, have been still left as open problems.

Furthermore, it is well known that the source correlation has an major impact on the system performance. The outage probability analysis for two correlated sources transmission over two independent channels utilizing Slepian-Wolf theorem is presented in [15], where the impact of source correlation is intensively studied. It is found that the *2nd* order diversity can be achieved only if the two sources are fully correlated, and the decay of the outage probability versus average signal-to-noise power ratio (SNR) asymptotically converges into no diversity if the two sources are not fully correlated. In the problem of correlated sources transmission over MARC, the impact of source correlation on the performance is still unknown. One of our focus points in on this issue.

In this paper, we investigate the network coding for correlated sources problem by considering a very simple form of WSNs, the MARC which consists of two source nodes, one relay node and one common destination node, as shown in Fig. 1. The data sequences obtained at the two source nodes S_1 and S_2 are assumed to be correlated, according to the property of WSNs. Furthermore, it is assumed that S_1 and S_2 can not communicate with each other. Instead, the relay node is used to assist the two sources to improve the probability of successful signal transmission of source information sequence to the destination. We assume decode-and-forward (DF) relaying strategy, and bit-wise XOR network coding is used at the relay node, therefore the information sent from the relay node can be regarded as additional redundancy. A JSCN decoding technique is then proposed to exploit the source correlation and the benefit of network coding simultaneously. The achievable compression rate region for the proposed system is derived according to the theorem for source coding with side information [16], [17]. Moreover, the performance limits are derived based on the achievable compression rate region and the impact of source correlation is investigated.

The rest of this paper is organized as follow. In Section II, the system model assumed in this paper is presented. Section III describes the proposed joint decoding strategy utilized at the destination, where the modified versions of boxplus operation [18] that take into account the source correlation are also derived. Section IV investigates the achievable compression rate region for the proposed system, based on the theorem for source coding with side information. The performance limit analysis, including limit in AWGN channels, outage proba-
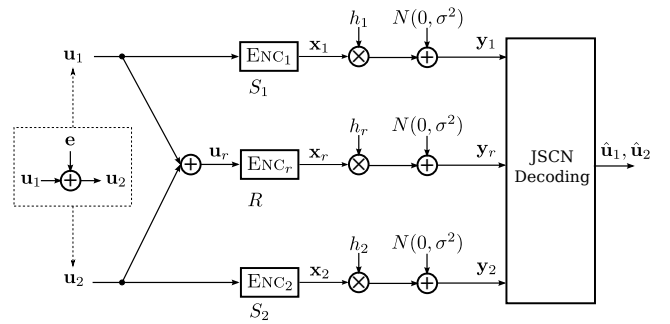
bility in Rayleigh fading channels and asymptotic tendency analysis, are presented in Section V. The simulation results for bit-error-rate (BER) and frame-error-rate (FER) performance in AWGN and block Rayleigh fading channels, respectively, are shown in Section VI. Finally, Section VII concludes this paper with some concluding remarks.

II. SYSTEM MODEL

The block diagram of the system considered in this paper is shown in Fig. 2. The binary data sequences $\mathbf{u}_1$ and $\mathbf{u}_2$, emitted from the two source nodes S_1 and S_2, respectively, are correlated with each other. The correlation between the sources can be described by the bit-flipping model [19] as follows. $\mathbf{u}_1$ is generated from an i.i.d. binary source with equiprobability, i.e., $\Pr(u_1^k = 0) = \Pr(u_1^k = 1) = 0.5$, where u_1^k denotes the k-th symbol of $\mathbf{u}_1$. $\mathbf{u}_2$ is then defined as $u_2^k = u_1^k \oplus e^k$ and $\Pr(e^k = 1) = 1 - \Pr(e^k = 0) = p$, where $\oplus$ denotes modulo-2 addition and p is the bit-flipping probability. We assume that the source-relay link is error free and therefore the relay can always successfully retrieve the data sequences obtained at the two source nodes.[1] Moreover, the transmissions from the two sources are assumed to be orthogonal due to time division transmission [20]. Consequently, three different time slots are assigned to the two source and relay nodes, since the relay is assumed to work in half-duplex mode.

At the source nodes S_1 and S_2, the data sequences $\mathbf{u}_1$ and $\mathbf{u}_2$ are first independently encoded by channel code ENC_1 and ENC_2, and then modulated by Binary Phase Shift Keying (BPSK) to obtain the modulated sequences $\mathbf{x}_1$ and $\mathbf{x}_2$, respectively. Then, at their dedicated time slots, each source node forwards the BPSK-modulated sequence, $\mathbf{x}_1$ or $\mathbf{x}_2$, to the relay and destination. As mentioned above, the source-relay link is assumed to be error-free. We demonstrate this concept in Fig. 2 by allowing direct access to $\mathbf{u}_1$ and $\mathbf{u}_2$ by the relay node. The relay node performs XOR operation on the perfectly recovered sequences $\mathbf{u}_1$ and $\mathbf{u}_2$ as $\mathbf{u}_r = \mathbf{u}_1 \oplus \mathbf{u}_2$. Then, the XORed sequence, $\mathbf{u}_r$, is encoded by channel code ENC_r and then modulated by BPSK to generate the signal sequence $\mathbf{x}_r$.

Note that we do not specify the channel codes ENC_1, ENC_2 and ENC_r here, and the simulation results using practical

---

[1] In this paper, the relay location is close enough to the sources such that the source-relay links can be assumed error free, with the help of proper error correction coding.
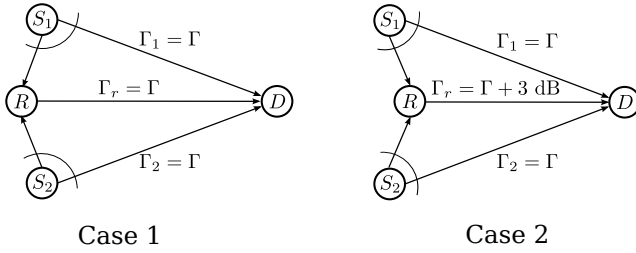
Fig. 3. Two different cases considered in this paper. In *case 1*, the relay and two source nodes keep the same distance to the destination node and thus the SNR of the three links are the same. In *case 2*, the SNR of the relay-destination link is increased by 3 dB.

Fig. 4. The proposed JSCN decoder for MARC. DEC_1, DEC_2 and DEC_r denotes the decoders of channel encoders ENC_1, ENC_2 and ENC_r used by S_1, S_2 and R, respectively.

coding chains are provided in Section VI-A. After receiving the signals from the two source nodes and the relay node, the destination performs JSCN decoding to retrieve the original data sequences sent from the two sources. This will be detailed in next section.

A. Channel Model

For notational simplicity, the link between S_1 and D is referred to as L_1. Similar definitions are applied to S_2 and R to get L_2 and L_r, respectively, as shown in Fig. 1. In this paper, the source-destination and relay-destination links are assumed to suffer from AWGN or frequency non-selective block Rayleigh fading. The received signal sequence at the destination can be expressed as

$$\mathbf{y}_i = h_i \cdot \mathbf{x}_i + \mathbf{n}_i, \qquad (1)$$

where $i = 1, 2, r$ corresponds to source nodes S_1, S_2 and relay node R, respectively. $\mathbf{n}_i$ and h_i represent zero mean i.i.d. complex Gaussian noise vector with variance σ^2 per dimension and the complex channel gain of L_i, respectively. With the block Raleigh fading assumption, the channel gain h_i remains constant over one block, but changes independently between the successive blocks. In this case, we can model h_i as zero-mean, circularly symmetric complex Gaussian random variables with unit variance. Hence, the magnitude $|h_i|$ is Rayleigh-distributed with $E[|h_i|^2] = 1$.

We assume that the two source nodes both have the same distance to the destination. Therefore, the average signal-to-noise ratios (SNRs) of both L_1 and L_2 are the same, i.e., $\Gamma_1 = \Gamma_2 = \Gamma$. The relay node can be located with the same distance to the destination as the source nodes, or closer to the destination. In this paper, we consider two different cases of the relay location, as shown in Fig. 3. In *Case 1*, the relay and two source nodes have the same distance to the destination node. In *Case 2*, the relay node is closer to the destination node than the two source nodes. Due to the geometric gain [15], the average SNR of L_r is larger than that with L_1 and L_2. Here, we assume the average SNR of the relay-destination link is 3 dB larger than Γ. Hence $\Gamma_r = \Gamma$ for *Case 1*, and $\Gamma_r = \Gamma + 3$ dB for *Case 2*.

III. JOINT DECODING STRATEGIES

A block diagram of the proposed JSCN decoder for MARC is illustrated in Fig. 4. The received signals at the destination
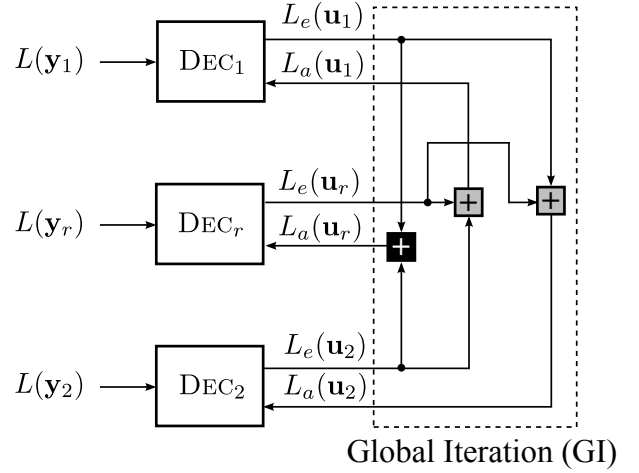
are first converted into log-likelihood ratios (LLRs) as [21]

$$L(y_i^k) = \ln \frac{\Pr(y_i^k | x_i^k = +1)}{\Pr(y_i^k | x_i^k = -1)} = \frac{2}{\sigma^2} \Re\{h_i^* \cdot y_i^k\}, \qquad (2)$$

where $i = 1, 2, r$ denotes S_1, S_2 and R, respectively. y_i^k and x_i^k are the k-th symbol of $\mathbf{y}_i$ and $\mathbf{x}_i$, respectively. h_i^* indicates the complex conjugation of h_i, and $\Re\{\cdot\}$ indicates the real part of its argument. The obtained LLR sequences $L(\mathbf{y}_1)$, $L(\mathbf{y}_2)$ and $L(\mathbf{y}_r)$ are then fed into three soft-in-soft-out (SISO) decoders DEC_1, DEC_2 and DEC_r, respectively, corresponding to ENC_1, ENC_2 and ENC_r. The extrinsic LLRs generated from DEC_1, DEC_2 and DEC_r are further exchanged via a Global Iteration (GI), as shown in Fig. 4.

As depicted in Fig. 2, XOR network coding is applied at the relay and the relationship between the data sequences transmitted from the two sources and relay node can be expressed as $\mathbf{u}_r = \mathbf{u}_1 \oplus \mathbf{u}_2$. In conventional MARC systems that does not take into account source correlation, joint network-channel (JNC) decoding is performed at the destination where the GI can be performed as

$$L_a(\mathbf{u}_r) = L_e(\mathbf{u}_1) \boxplus L_e(\mathbf{u}_2) = \ln \frac{1 + \exp[L_e(\mathbf{u}_1) + L_e(\mathbf{u}_2)]}{\exp[L_e(\mathbf{u}_1)] + \exp[L_e(\mathbf{u}_2)]}, \qquad (3)$$

with $\boxplus$ denoting the boxplus operation which is equivalent to the XOR operation in the LLR domain [18], [22]. $L_e(\mathbf{u}_1)$ and $L_e(\mathbf{u}_2)$ denote the *extrinsic* LLRs generated from DEC_1 and DEC_2, respectively, and $L_a^R(\mathbf{u}_r)$ denotes the *a priori* LLRs fed into DEC_r. The *a priori* LLRs fed into DEC_1 and DEC_2, which are denoted as $L_a(\mathbf{u}_1)$ and $L_a(\mathbf{u}_2)$, respectively, can be obtained in the same way.

If the two correlated sources are transmitted to the destination node without the help of the relay node, only the source correlation can be exploited at the destination. In this case, joint source-channel (JSC) decoding can be performed at the destination to exploit the source correlation. DEC_1 and DEC_2 can exchange their extrinsic information via the f_c function

proposed in [23], [24] as

$$L_a(\mathbf{u}_1) = f_c(L_e(\mathbf{u}_2), p) = \ln \frac{p + (1-p) \cdot \exp[L_e(\mathbf{u}_2)]}{(1-p) + p \cdot \exp[L_e(\mathbf{u}_2)]}. \tag{4}$$

The *a priori* LLRs $L_a(\mathbf{u}_2)$ that fed into DEC_2 can be obtained in the same way.

In our proposed system, the two sources are correlated and XOR network coding is performed at the relay node. In order to take into account the correlation knowledge between $\mathbf{u}_1$ and $\mathbf{u}_2$, as well as with the assistance of network coding, modified versions of the boxplus operation are derived to perform JSCN at the destination, which is detailed in the next sub-section. Finally, after sufficient iterations, hard decision is made based on the output of D_1 and D_2 to get the estimate of $\mathbf{u}_1$ and $\mathbf{u}_2$, respectively.

A. Modified Boxplus Operation for Relay Node

Since the correlation between $\mathbf{u}_1$ and $\mathbf{u}_2$ is modeled by the bit-flipping model, it is quite straightforward to obtain the following equations, according to [19], [23]:

$$\begin{aligned}
\Pr(u_r^k = 0) &= \Pr(u_1^k = 0, u_2^k = 0) + \Pr(u_1^k = 1, u_2^k = 1) \\
&= \Pr(u_1^k = 0) \cdot \Pr(u_2^k = 0) \cdot (1-p) \\
&\quad + \Pr(u_1^k = 1) \cdot \Pr(u_2^k = 1) \cdot (1-p),
\end{aligned} \tag{5}$$

$$\begin{aligned}
\Pr(u_r^k = 1) &= \Pr(u_1^k = 0, u_2^k = 1) + \Pr(u_1^k = 1, u_2^k = 0) \\
&= \Pr(u_1^k = 0) \cdot \Pr(u_2^k = 1) \cdot p \\
&\quad + \Pr(u_1^k = 1) \cdot \Pr(u_2^k = 0) \cdot p,
\end{aligned} \tag{6}$$

where u_1^k, u_2^k and u_r^k denote the k-th symbol of $\mathbf{u}_1$, $\mathbf{u}_2$ and $\mathbf{u}_r$, respectively. With (5) and (6), the LLR for u_r^k can be obtained as

$$\begin{aligned}
L(u_r^k) &= L(u_1^k) \boxplus_r L(u_2^k) = \ln \frac{\Pr(u_r^k = 0)}{\Pr(u_r^k = 1)} \\
&= \ln \frac{1-p}{p} + \ln \frac{1 + \exp[L(u_1^k) + L(u_2^k)]}{\exp[L(u_1^k)] + \exp[L(u_2^k)]},
\end{aligned} \tag{7}$$

where $\boxplus_r$ denotes the modified version of the boxplus operation for updating the LLR values of $\mathbf{u}_r$, based on the LLR values of $\mathbf{u}_1$ and $\mathbf{u}_2$, which corresponds to the black box in Fig. 4. It can be observed from (7) that the correlation between $\mathbf{u}_1$ and $\mathbf{u}_2$ has been exploited.

B. Modified Boxplus Operation for Source Node

The LLR updating rules for the source nodes are different from that of the relay node. We first demonstrate the derivation process for the LLR updating function for the signal transmitted from S_1. In the same way as $\boxplus_r$ was derived, we can obtain the following equations:

$$\begin{aligned}
\Pr(u_1^k = 0) &= \Pr(u_r^k = 0, u_2^k = 0) + \Pr(u_r^k = 1, u_2^k = 1) \\
&= \Pr(u_r^k = 0) \cdot \Pr(u_2^k = 0) \cdot (1-p) \\
&\quad + \Pr(u_r^k = 1) \cdot \Pr(u_2^k = 1) \cdot p,
\end{aligned} \tag{8}$$

$$\begin{aligned}
\Pr(u_1^k = 1) &= \Pr(u_r^k = 0, u_2^k = 1) + \Pr(u_r^k = 1, u_2^k = 0) \\
&= \Pr(u_r^k = 0) \cdot \Pr(u_2^k = 1) \cdot (1-p) \\
&\quad + \Pr(u_r^k = 1) \cdot \Pr(u_2^k = 0) \cdot p,
\end{aligned} \tag{9}$$

where u_1^k, u_2^k and u_r^k denote the k-th symbol of $\mathbf{u}_1$, $\mathbf{u}_2$ and $\mathbf{u}_r$, respectively. It can be obtained from (8) and (9) that the LLR updating function for u_1^k is

$$\begin{aligned}
L(u_1^k) &= L(u_r^k) \boxplus_s L(u_2^k) = \ln \frac{\Pr(u_1^k = 0)}{\Pr(u_1^k = 1)} \\
&= \ln \frac{p + (1-p) \cdot \exp[L(u_r^k) + L(u_2^k)]}{(1-p) \cdot \exp[L(u_r^k)] + p \cdot \exp[L(u_2^k)]},
\end{aligned} \tag{10}$$

where $\boxplus_s$ denotes the modified version of boxplus operation for updating the LLR values of $\mathbf{u}_1$, which corresponds to the gray box in Fig. 4. The LLR updating function for S_2 can be derived in the same way.

Note that in the case the two sources are uncorrelated ($p = 0.5$), the modified boxplus operations, $\boxplus_r$ and $\boxplus_s$, are both equivalent to the original boxplus operation $\boxplus$. Furthermore, if the relay node does not help in the decoding process, corresponding to the case $L_e^R(\mathbf{u}_r) = 0$, the modified boxplus operation $\boxplus_s$ is equivalent to the original f_c function [23], [24].

In summary, the GI operation of the proposed decoder, as shown in Fig. 4, can be expressed as:

$$\begin{cases}
L_a(\mathbf{u}_r) = L_e(\mathbf{u}_1) \boxplus_r L_e(\mathbf{u}_2), \\
L_a(\mathbf{u}_1) = L_e(\mathbf{u}_r) \boxplus_s L_e(\mathbf{u}_2), \\
L_a(\mathbf{u}_2) = L_e(\mathbf{u}_r) \boxplus_s L_e(\mathbf{u}_1).
\end{cases} \tag{11}$$

By performing GI operations with the modified boxplus functions, the extrinsic LLRs are updated, which take into account both the impact of the source correlation and XOR network coding at the relay.

IV. ACHIEVABLE COMPRESSION RATE REGION ANALYSIS

Due to the XOR operation at the relay node, the achievable compression rate for $\mathbf{u}_1$ and $\mathbf{u}_2$ may not only be determined by the Slepian-Wolf theorem. However, in MARC considered in our system, the destination only aims to recover the data sequence $\mathbf{u}_1$ and $\mathbf{u}_2$, which are sent from S_1 and S_2, respectively (we are not interested in the sequence transmitted from the relay, but we only use it). The data sequence $\mathbf{u}_r$ sent from the relay can be regarded as additional redundancy and are used to enhance the performance of the system. Therefore, the theorem for source coding with side information [16], [17] can be used for determining the achievable compression rate region for MARC with correlated sources.

Assume that the channel codes, ENC_1, ENC_2, and ENC_r, are close-limit achieving, corresponding to their rates (i.e., their BER performance curves exhibit clear threshold at the SNR values very close to the Shannon limit). According to the theorem for source coding with side information, the achievable compression rate region is given by

$$\begin{cases}
R_1 &\geq H(\mathbf{u}_1 | \mathbf{u}_2, \hat{\mathbf{u}}_r), \\
R_2 &\geq H(\mathbf{u}_2 | \mathbf{u}_1, \hat{\mathbf{u}}_r), \\
R_1 + R_2 &\geq H(\mathbf{u}_1, \mathbf{u}_2 | \hat{\mathbf{u}}_r), \\
R_r &\geq I(\mathbf{u}_r; \hat{\mathbf{u}}_r),
\end{cases} \tag{12}$$

where R_1, R_2 and R_r are the compression rates for $\mathbf{u}_1$, $\mathbf{u}_2$ and $\mathbf{u}_r$, respectively. $\hat{\mathbf{u}}_r$ is the estimate of $\mathbf{u}_r$ at the final output, which serves as side information at D. $H(\mathbf{u}_1 | \mathbf{u}_2, \hat{\mathbf{u}}_r)$ denotes
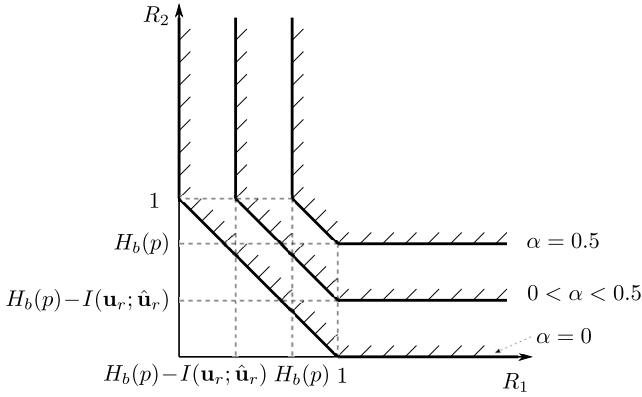
Fig. 5. The achievable compression rate region for R_1 and R_2. α is the error probability between $\mathbf{u}_r$ and $\hat{\mathbf{u}}_r$.

Fig. 6. The achievable compression rate region of the proposed system.

the entropy of $\mathbf{u}_1$, conditioned on $\mathbf{u}_2$ and $\hat{\mathbf{u}}_r$. Similar definitions apply to $H(\mathbf{u}_2|\mathbf{u}_1, \hat{\mathbf{u}}_r)$ and $H(\mathbf{u}_1, \mathbf{u}_2|\hat{\mathbf{u}}_r)$. $I(\mathbf{u}_r; \hat{\mathbf{u}}_r)$ denotes the mutual information between $\mathbf{u}_r$ and $\hat{\mathbf{u}}_r$.

Since D does not aim to successfully decode $\mathbf{u}_r$, $\hat{\mathbf{u}}_r$ may contain some errors. The relationship between binary data sequences $\mathbf{u}_r$ and $\hat{\mathbf{u}}_r$ can also be expressed as a bit-flipping model with a error probability $\alpha, \alpha \in [0, 0.5]$. After some mathematical manipulations, we have

$$\begin{cases} H(\mathbf{u}_2|\mathbf{u}_1, \hat{\mathbf{u}}_r) = H_b(p) - I(\mathbf{u}_r; \hat{\mathbf{u}}_r), \\ H(\mathbf{u}_1|\mathbf{u}_2, \hat{\mathbf{u}}_r) = H_b(p) - I(\mathbf{u}_r; \hat{\mathbf{u}}_r), \\ H(\mathbf{u}_1, \mathbf{u}_2|\hat{\mathbf{u}}_r) = 1 + H_b(p) - I(\mathbf{u}_r; \hat{\mathbf{u}}_r), \\ I(\mathbf{u}_r, \hat{\mathbf{u}}_r) = H_b(\alpha + p - 2\alpha p) - H_b(\alpha), \end{cases} \quad (13)$$

where $H_b(\cdot)$ is the binary entropy function with definition $H_b(x) = -x \cdot \log_2(x) - (1-x) \cdot \log_2(1-x)$.

According to (13), the achievable compression rate region is determined by the source correlation p and the error probability α. For a given p value, the achievable compression rate region is decided only by α. First we focus on the achievable compression rate region of R_1 and R_2. If $\alpha = 0.5$, the estimate $\hat{\mathbf{u}}_r$ of $\mathbf{u}_r$ after decoding does not contain any information of $\mathbf{u}_r$ and hence can not be utilized in the joint decoding process. In this case, the achievable compression rate region for R_1 and R_2 is $R_1 \geq H_b(p)$, $R_2 \geq H_b(p)$ and $R_1 + R_2 \geq 1 + H_b(p)$, which is the region surrounded by a polygon as shown in Fig. 5. It can be seen that the region is the same as that determined by the Slepian-Wolf theorem for two correlated sources. If $\alpha = 0$, $\mathbf{u}_r$ can be successfully decoded at the destination. Hence, the achievable compression rate region for R_1 and R_2 becomes $R_1 \geq 0$, $R_2 \geq 0$ and $R_1 + R_2 \geq 1$, as depicted in Fig 5. In this case, the achievable compression rate region for R_1 and R_2 is the largest. If $0 < \alpha < 0.5$, the achievable compression rate region for R_1 and R_2 is between these two extreme cases, which is also shown in the same figure.

The error probability α between $\mathbf{u}_r$ and $\hat{\mathbf{u}}_r$, is determined by the quality of L_r. Since we assume the channel codes ENC_1, ENC_2 and ENC_r are close-limit achieving, obviously, the minimum compression rate for R_r is $R_{r,min} = I(\mathbf{u}_r; \hat{\mathbf{u}}_r)$. Taking R_r into the account, the achievable compression rate region for the proposed system can be determined, which is
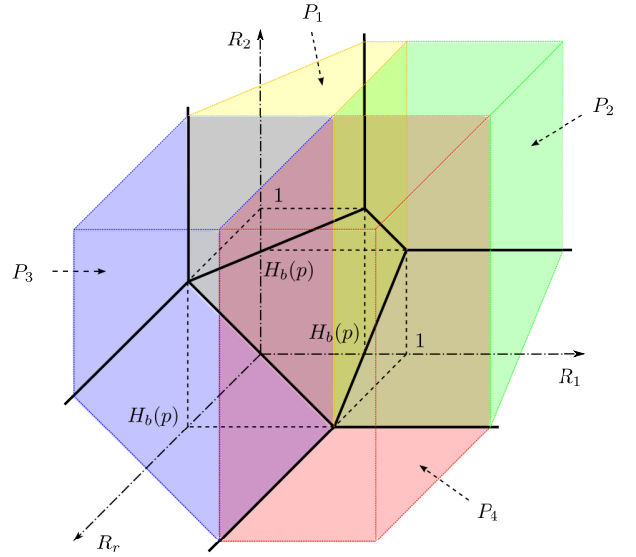
the 3-dimensional (3D) space surrounded by the polyhedron, as shown in Fig. 6.

V. PERFORMANCE LIMIT ANALYSIS

A. Relationship Between Compression Rates and Its Corresponding Channel SNRs

It should be emphasized here that, in the system considered in this paper, *source coding for compression is performed neither at S_1, S_2 nor R*. Instead, the correlation knowledge among $\mathbf{u}_1$, $\mathbf{u}_2$ and $\mathbf{u}_r$ are exploited at D to enhance the error correction capability of the system. According to the Shannon's separation theorem, if the *total* information transmission rates over independent channels satisfy [23]

$$\begin{cases} R_1 R_{c1} & \leq & C(\Gamma_1), \\ R_2 R_{c2} & \leq & C(\Gamma_2), \\ R_r R_{cr} & \leq & C(\Gamma_r), \end{cases} \quad (14)$$

the message error probability can be infinitesimally reduced. Here, R_{c1}, R_{c2} and R_{cr} are the spectrum efficiency of the transmission chain, including the channel coding scheme and the modulation multiplicity of the links L_1, L_2 and L_r, respectively. $C(\Gamma_1)$, $C(\Gamma_2)$ and $C(\Gamma_r)$ denote the channel capacity of the links L_1, L_2 and L_r, respectively.[2]

In the theoretical analysis, we assume that the channel codes ENC_1, ENC_2 and ENC_r are close-capacity achieving, therefore we only consider the equality of (14). The relationship between the compression rate R_i and its corresponding channel SNR Γ_i is given by

$$R_i = \Phi_i(\Gamma_i) = \frac{C(\Gamma_i)}{R_{ci}}, \quad (15)$$

with its reverse function

$$\Gamma_i = \Phi_i^{-1}(R_i) = C^{-1}(R_i R_{ci}), \quad (16)$$

[2]$C(x) = \frac{N_D}{2} \log_2(1 + \frac{2x}{N_D})$, with its inverse function $C^{-1}(x) = \frac{N_D}{2}(2^{\frac{2x}{N_D}} - 1)$, where N_D denotes the dimension of the channel input.
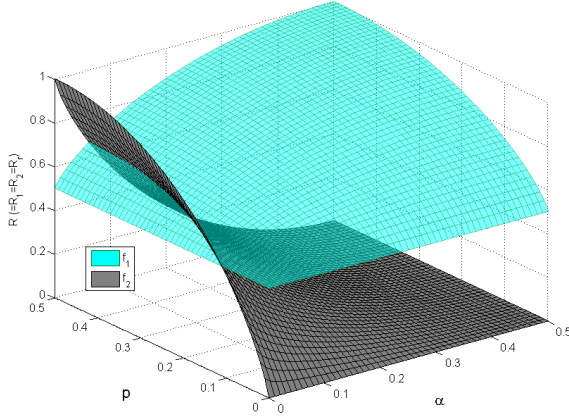
Fig. 7. The minimum compression rate of our system in *case 1*. p denotes the bit-flipping probability between the two sources. α denotes the error probability between $\mathbf{u}_r$ and $\hat{\mathbf{u}}_r$.

where $i = 1, 2, r$ and $C^{-1}(\cdot)$ denotes the inverse function of channel capacity.

B. Limits in AWGN Channels

1) Case 1 Relay Location: In this case, the instantaneous SNR of L_1, L_2 and L_r are the same, i.e., $\Gamma_1 = \Gamma_2 = \Gamma_r$. Assuming that the spectrum efficiency of L_1, L_2 and L_r are also the same, i.e., $R_{c1} = R_{c2} = R_{cr}$, we can obtain $R_1 = R_2 = R_r = R$ according to (15). Then the compression rate R is determined by

$$\begin{cases} R \geq \frac{1}{2}[1 + H_b(\alpha) + H_b(p) - H_b(\alpha + p - 2\alpha p)] = f_1(\alpha, p), \\ R \geq H_b(\alpha + p - 2\alpha p) - H_b(\alpha) = f_2(\alpha, p). \end{cases}$$
$$(17)$$

The minimum compression rate R_{min} is achieved on the intersection of $f_1(\alpha, p)$ and $f_2(\alpha, p)$, as shown in Fig. 7. It can be seen from this figure that if $H_b(p) \leq 0.5$, R_{min} is determined by $f_1(\alpha, p)$ only. By combining (14) and (17), we can obtain the performance limit of our system in AWGN channels for *Case 1*.

2) Case 2 Relay Location: In this case, $\Gamma_r = \Gamma_1 + 3$ dB, however, the relationship between R_1, R_2 and R_r does not have to be explicitly identified. However, the performance limit of our system can be calculated by combining (12), (13) and (14).

C. Outage Probability Analysis in Rayleigh Fading Channels

According to [15], the outage probability of the proposed system can be derived once the achievable compression rate region is determined. As described in Section II-A, the instantaneous SNR of L_i is denoted by $\gamma_i = |h_i|^2 E_{s,i}/2\sigma^2$, where $E_{s,i}$ represents the per-symbol signal power of L_i and $i = 1, 2, r$ corresponds to S_1, S_2 and D, respectively. According to (15), the relationship between R_i and its corresponding instantaneous SNR of L_i is $R_i = \Phi_i(\gamma_i)$, and $\gamma_i = \Phi_i^{-1}(R_i)$ $i = 1, 2, r$.

As shown in Fig. 6, the entire rate region for the proposed system can be divided into 4 parts, with P_j, $j =$

$1, 2, 3, 4$, representing the probability that the rate combination (R_1, R_2, R_r) falls into Part j. As mentioned in Section IV, α is determined by the quality of L_r and the minimum value for R_r is $R_{r,min} = I(\mathbf{u}_r, \hat{\mathbf{u}}_r)$. If the instantaneous SNR of L_r, γ_r, falls under a certain threshold, then $\hat{\mathbf{u}}_r \neq \mathbf{u}_r$ at D after decoding. In this case, $R_{r,min}$ ranges from 0 to $H(p)$ and the achievable rate region is represented by P_1 and P_2. On the contrary, if γ_r is above this certain threshold, then $\hat{\mathbf{u}}_r = \mathbf{u}_r$ at D after decoding. In this case, $R_{r,min} = H(p)$ and the achievable rate region is represented by P_3 and P_4.

If (R_1, R_2, R_r) falls into the achievable rate region, $\mathbf{u}_1$ and $\mathbf{u}_2$ can be successfully decoded at D. Hence, the outage event happens when (R_1, R_2, R_r) falls outside the achievable rate region, and the outage probability of the proposed system can be expressed as

$$P_{out} = 1 - P_1 - P_2 - P_3 - P_4, \quad (18)$$

where

$$\begin{aligned} P_1 &= \Pr\{0 \leq R_r \leq H_b(p), H_b(p) - I(\mathbf{u}_r, \hat{\mathbf{u}}_r) \leq R_1 \leq 1, \\ &\quad R_1 + R_2 \geq 1 + H_b(p) - I(\mathbf{u}_r, \hat{\mathbf{u}}_r)\} \\ &= \Pr\{\Phi_r^{-1}(0) \leq \gamma_r \leq \Phi_r^{-1}[H_b(p)], \\ &\quad \Phi_1^{-1}[H_b(p) - \Phi_r(\gamma_r)] \leq \gamma_1 \leq \Phi_1^{-1}(1), \\ &\quad \gamma_2 \geq \Phi_2^{-1}[1 + H_b(p) - \Phi_r(\gamma_r) - \Phi_1(\gamma_1)]\}, \end{aligned}$$
$$(19)$$

$$\begin{aligned} P_2 &= \Pr\{0 \leq R_r \leq H_b(p), R_1 \geq 1, R_2 \geq H_b(p) - I(\mathbf{u}_r, \hat{\mathbf{u}}_r)\} \\ &= \Pr\{\Phi_r^{-1}(0) \leq \gamma_r \leq \Phi_r^{-1}[H_b(p)], \gamma_1 \geq \Phi_1^{-1}(1), \\ &\quad \gamma_2 \geq \Phi_2^{-1}[H_b(p) - \Phi_r(\gamma_r)]\}, \end{aligned}$$
$$(20)$$

$$\begin{aligned} P_3 &= \Pr\{R_r \geq H_b(p), 0 \leq R_1 \leq 1, R_1 + R_2 \geq 1\} \\ &= \Pr\{\gamma_r \geq \Phi_r^{-1}[H_b(p)], \Phi_1^{-1}(0) \leq \gamma_1 \leq \Phi_1^{-1}(1), \quad (21) \\ &\quad \gamma_2 \geq \Phi_2^{-1}[1 - \Phi_1(\gamma_1)]\}, \end{aligned}$$

and

$$\begin{aligned} P_4 &= \Pr\{R_r \geq H_b(p), R_1 \geq 1, R_2 \geq 0\} \\ &= \Pr\{\gamma_r \geq \Phi_r^{-1}[H_b(p)], \gamma_1 \geq \Phi_1^{-1}(1), \gamma_2 \geq \Phi_2^{-1}(0)\}. \end{aligned}$$
$$(22)$$

Since L_1, L_2 and L_r are suffering from statistically independent block Rayleigh fading, the joint probability density function (pdf) of the instantaneous SNRs can be expressed as $p(\gamma_r, \gamma_1, \gamma_2) = p(\gamma_r) \cdot p(\gamma_1) \cdot p(\gamma_2)$, where

$$p(\gamma_i) = \frac{1}{\Gamma_i} \exp(-\frac{\gamma_i}{\Gamma_i}), \ i = 1, 2, r. \quad (23)$$

Here $\Gamma_i = E_{s,i}/2\sigma^2$ represents the average SNR of L_i. With (23), the probabilities P_1, P_2, P_3 and P_4 can be further

expressed as triple integrals, as:

$$P_1 = \int_{\Phi_r^{-1}(0)}^{\Phi_r^{-1}[H_b(p)]} d\gamma_r \int_{\Phi_1^{-1}[H_b(p)-\Phi_r(\gamma_r)]}^{\Phi_1^{-1}(1)} d\gamma_1$$

$$\cdot \int_{\Phi_2^{-1}[1+H_b(p)-\Phi_r(\gamma_r)-\Phi_1(\gamma_1)]}^{\Phi_2^{-1}(\infty)} p(\gamma_r)p(\gamma_1)p(\gamma_2)d\gamma_2$$

$$= \int_{\Phi_r^{-1}(0)}^{\Phi_r^{-1}[H_b(p)]} d\gamma_r \int_{\Phi_1^{-1}[H_b(p)-\Phi_r(\gamma_r)]}^{\Phi_1^{-1}(1)}$$

$$p(\gamma_r)p(\gamma_1)\left[-\exp(-\frac{\gamma_2}{\Gamma_2})\right]_{\Phi_2^{-1}[1+H_b(p)-\Phi_r(\gamma_r)-\Phi_1(\gamma_1)]}^{\Phi_2^{-1}(\infty)} d\gamma_1$$

$$= \frac{1}{\Gamma_r\Gamma_1}\int_{\Phi_r^{-1}(0)}^{\Phi_r^{-1}[H_b(p)]} d\gamma_r \int_{\Phi_2^{-1}[1+H_b(p)-\Phi_r(\gamma_r)-\Phi_1(\gamma_1)]}^{\Phi_2^{-1}(1)}$$

$$\exp\left\{-\frac{\gamma_r}{\Gamma_r}-\frac{\gamma_1}{\Gamma_1}-\frac{\Phi_2^{-1}[1+H_b(p)-\Phi_r(\gamma_r)-\Phi_1(\gamma_1)]}{\Gamma_2}\right\} d\gamma_1, \tag{24}$$

$$P_2 = \int_{\Phi_r^{-1}(0)}^{\Phi_r^{-1}[H_b(p)]} d\gamma_r \int_{\Phi_1^{-1}(1)}^{\Phi_1^{-1}(\infty)} d\gamma_1 \int_{\Phi_2^{-1}[H_b(p)-\Phi_r(\gamma_r)]}^{\Phi_2^{-1}(\infty)}$$

$$p(\gamma_r)p(\gamma_1)p(\gamma_2)d\gamma_2$$

$$= \int_{\Phi_r^{-1}(0)}^{\Phi_r^{-1}[H_b(p)]} p(\gamma_r)\cdot\left[-\exp(-\frac{\gamma_1}{\Gamma_1})\right]_{\Phi_1^{-1}(1)}^{\Phi_1^{-1}(\infty)}$$

$$\cdot \left[-\exp(\frac{\gamma_2}{\Gamma_2})\right]_{\Phi_2^{-1}[H_b(p)-\Phi_r(\gamma_r)]}^{\Phi_2^{-1}(\infty)} d\gamma_r$$

$$= \frac{1}{\Gamma_r}\exp\left[-\frac{\Phi_1^{-1}(1)}{\Gamma_1}\right]\int_{\Phi_r^{-1}(0)}^{\Phi_r^{-1}[H_b(p)]}$$

$$\exp\left\{-\frac{\gamma_r}{\Gamma_r}-\frac{\Phi_2^{-1}[H_b(p)-\Phi_r(\gamma_r)]}{\Gamma_2}\right\} d\gamma_r, \tag{25}$$

$$P_3 = \int_{\Phi_r^{-1}[H_b(p)]}^{\Phi_r^{-1}(\infty)} d\gamma_r \int_{\Phi_1^{-1}(0)}^{\Phi_1^{-1}(1)} d\gamma_1$$

$$\cdot \int_{\Phi_2^{-1}[1-\Phi_1(\gamma_1)]}^{\Phi_2^{-1}(\infty)} p(\gamma_r)p(\gamma_1)p(\gamma_2)d\gamma_2$$

$$= \int_{\Phi_1^{-1}(0)}^{\Phi_1^{-1}(1)} \left[-\exp(-\frac{\gamma_r}{\Gamma_r})\right]_{\Phi_r^{-1}[H_b(p)]}^{\Phi_r^{-1}(\infty)}$$

$$\cdot p(\gamma_1)\cdot\left[-\exp(\frac{\gamma_2}{\Gamma_2})\right]_{\Phi_2^{-1}[1-\Phi_1(\gamma_1)]}^{\Phi_2^{-1}(\infty)} d\gamma_1$$

$$= \frac{1}{\Gamma_1}\exp\left\{-\frac{\Phi_r^{-1}[H_b(p)]}{\Gamma_r}\right\}$$

$$\cdot \int_{\Phi_1^{-1}(0)}^{\Phi_1^{-1}(1)} \exp\left\{-\frac{\gamma_1}{\Gamma_1}-\frac{\Phi_2^{-1}[1-\Phi_1(\gamma_1)]}{\Gamma_2}\right\} d\gamma_1, \tag{26}$$

and

$$P_4 = \int_{\Phi_r^{-1}[H_b(p)]}^{\Phi_r^{-1}(\infty)} d\gamma_r \int_{\Phi_1^{-1}(1)}^{\Phi_1^{-1}(\infty)} d\gamma_1$$

$$\cdot \int_{\Phi_2^{-1}(0)}^{\Phi_2^{-1}(\infty)} p(\gamma_r)p(\gamma_1)p(\gamma_2)d\gamma_2$$

$$= \left[-\exp(-\frac{\gamma_r}{\Gamma_r})\right]_{\Phi_r^{-1}[H_b(p)]}^{\Phi_r^{-1}(\infty)} \cdot \left[-\exp(-\frac{\gamma_1}{\Gamma_1})\right]_{\Phi_1^{-1}(1)}^{\Phi_1^{-1}(\infty)}$$

$$\cdot \left[-\exp(-\frac{\gamma_2}{\Gamma_2})\right]_{\Phi_2^{-1}(0)}^{\Phi_2^{-1}(\infty)}$$

$$= \exp\left[-\frac{\Phi_1^{-1}(1)}{\Gamma_1}\right]\exp\left\{-\frac{\Phi_r^{-1}[H_b(p)]}{\Gamma_r}\right\}. \tag{27}$$

Except for P_4, the derivation for the explicit expressions of the integrals in (24), (25) and (26) may not be possible. Instead, a numerical method is used to calculate the values of P_1, P_2 and P_3.

D. Asymptotic Tendency Analysis

First we evaluate the outage probability of the proposed system when the two sources are fully correlated ($p = 0$). In this case, we have $H_b(p) = 0$. The integral range of γ_r in (24) and (25) are both from 0 to 0, which means $P_1 = P_2 = 0$. Moreover, we can have

$$\exp\left\{-\frac{\Phi_r^{-1}[H_b(p)]}{\Gamma_r}\right\} = 1. \tag{28}$$

and outage probability becomes

$$P_{out,p=0} = 1 - P_1 - P_2 - P_3 - P_4$$

$$= 1 - \exp\left[-\frac{\Phi_1^{-1}(1)}{\Gamma_1}\right]$$

$$- \frac{1}{\Gamma_1}\int_{\Phi_1^{-1}(0)}^{\Phi_1^{-1}(1)} \exp\left\{-\frac{\gamma_1}{\Gamma_1}-\frac{\Phi_2^{-1}[1-\Phi_1(\gamma_1)]}{\Gamma_2}\right\} d\gamma_1. \tag{29}$$

It is found from (29) that if the two sources are fully correlated, the outage probability is only determined by the quality of L_1 and L_2.

As mentioned in Section II-A, we assume $\Gamma_1 = \Gamma_2$ and Γ_r is Δ dB larger than Γ_1, i.e., $\Gamma_r = \Gamma_1 \cdot 10^{\Delta/10}$. In this paper, we only considered the case when $\Delta = 0$ (*Case 1*) and that when $\Delta = 3$ (*Case 2*). Next the outage probability of the proposed system is evaluated when Δ approaches infinity. For given Γ_1, when $\Delta \to \infty$, $\frac{1}{\Gamma_r} = \frac{1}{\Gamma_1 \cdot 10^{\Delta/10}} \to 0$. According to (24) and (25), we have $P_1 = P_2 = 0$. Furthermore, as $\Delta \to \infty$, it is found that

$$\exp\left\{-\frac{\Phi_r^{-1}[H_b(p)]}{\Gamma_r}\right\} = \exp\left\{-\frac{\Phi_r^{-1}[H_b(p)]}{\Gamma_1 \cdot 10^{\Delta/10}}\right\} \to 1. \tag{30}$$

Obviously, the outage probability of the proposed system when $\Delta \to \infty$ is the same as in the case where the two sources are fully correlated, as:
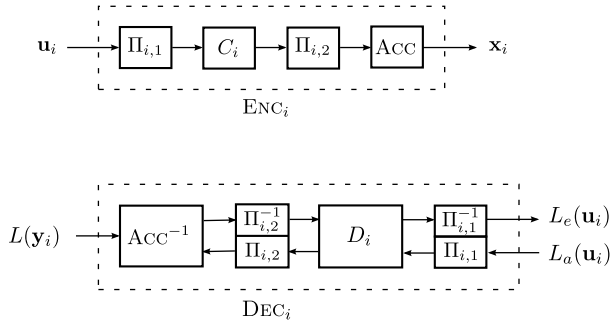
$$P_{out,\Delta\to\infty} = P_{out,p=0}. \tag{31}$$

Fig. 8. Coding and decoding structure for ENC_i and DEC_i, respectively, $i = 1, 2, r$. D_i is the decoder for C_i. ACC and ACC^{-1} denote the accumulator and the decoder for accumulator, respectively.

VI. Numerical Results

A. Code Structure[3]

In the theoretical analysis, we assume that the channel codes ENC_1, ENC2_2 and ENC_r all exhibit close-limit performance. However, in this section, we use serially concatenated codes (SCC) for ENC_i, $i = 1, 2, r$. The outer code in SCC is half-rate memory-1 non-recursive non-systematic convolutional (NRNSC) code [24] with generator polynomial $(3, 2)_8$, and the inner code is doped accumulator [24] with doping rate Q_i, $i = 1, 2, r$, as shown in Fig. 8. Therefore, $R_{c1} = R_{c2} = R_{cr} = 1/2$. The decoding chain for ENC_i, DEC_i, is also shown in the same figure, which is denoted as Local Iteration (LI). In the LI, Bahl-Cocke-Jelinek-Raviv (BCJR) algorithm is used both in D_i and ACC^{-1}. It has been shown in [24] that even with this simple SCC code, still excellent performance can be achieved. In our simulations, the doping rates were set as $Q_1 = Q_2 = Q_R = 1$. We performed GI after every LI, and the whole process was repeated 20 times.

B. BER Performance Evaluation in AWGN Channels

BER performance evaluation for the proposed system with several representative p values are provided in this subsection. In our simulations, the frame length is set at $10,000$ bits, and 1000 different frames were transmitted from each source node. To demonstrate the performance gains achieved by the exploitation of the correlation between sources, the BER curve of conventional XOR network coding based MARC that does not exploit source correlation are also provided, which is denoted by "NC". In this conventional MARC, the original boxplus operation of (3) is used for extrinsic information exchange during the joint channel-network decoding process. As a reference, the BER performance of the system that does not utilize network coding (without relay node) but only exploits the source correlation by using the f_c function of (4) is also provided in the same figure, which is denoted as "SC".

The BER performance of the proposed system in *Case 1* is depicted in Fig. 9. It can be observed that the BER performance of our JSCN coding scheme provides significant gain over both "SC" and "NC". It should be emphasized here

[3]In the simulations, we assumed that the bit-flipping probability p is known to the decoder. However, the p value can be estimated only at the destination, and the algorithm is detailed in [23], [24].
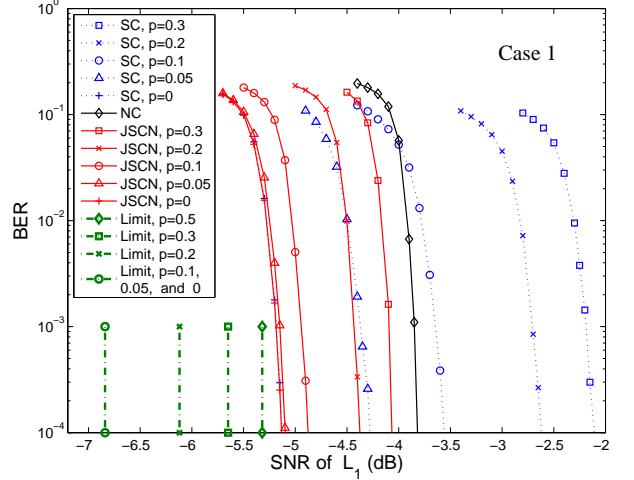

Fig. 9. BER performance of the proposed JSCN technique for MARC with correlated sources in *Case 1*, with respect to the SNR of L_1. Different source correlation are considered.
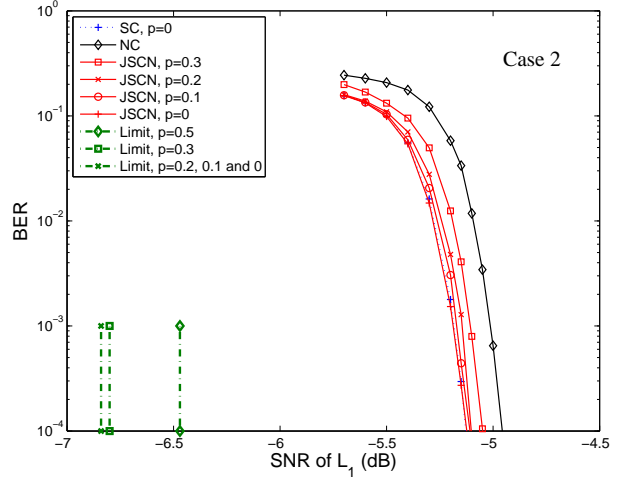

Fig. 10. BER performance of the proposed JSCN technique for MARC with correlated sources in *Case 2*, with respect to the SNR of L_1. Different source correlation are considered.

that as the source correlation becomes larger, the gain over "NC" increases while the gain over "SC" decreases. However, even with a relative small p value ($p = 0.05$), still considerable gains can be achieved over "SC". If the two sources are fully correlated ($p = 0$), the BER performance of the proposed JSCN technique and "SC" are the same. Because in this case, the modified boxplus operation $\boxplus_s$ used in JSCN and the f_c function used in "SC" become equivalent, as described in Section III.

Fig. 10 shows the BER performance of the proposed system in *Case 2*. As can be seen from the figure, if $p = 0$, the BER performance of the proposed system is the same as that in *Case 1*. This is because the modified boxplus operation $\boxplus_s$ becomes equivalent to the f_c function used in "SC" if $p = 0$, which means $\boxplus_s$ does not take any help from the relay node. For $p = 0.3, 0.2$ and 0.1, the performance are quite close to

TABLE I
PERFORMANCE GAINS AND GAPS TO THE THEORETICAL LIMITS FOR THE PROPOSED JSCN CODING SCHEME, AT THE BER LEVEL OF 10^{-4}.

| | | p | Limits (dB) | Gains (dB) | | Gaps (dB) |
				over NC	over SC	
Case 1	NC	0.5	-5.32	-	-	1.5
	JSCN	0.3	-5.65	0.25	1.96	1.58
		0.2	-6.12	0.55	1.75	1.75
		0.1	-6.84	1.06	1.32	1.96
		0.05	-6.84	1.17	0.81	1.75
		0	-6.84	1.31	0	1.71
Case 2	NC	0.5	-6.47	-	-	1.52
	JSCN	0.3	-6.80	0.1	2.94	1.75
		0.2	-6.84	0.15	2.48	1.74
		0.1	-6.84	0.16	1.55	1.73
		0	-6.84	0.18	0	1.71

that with $p = 0$.

The performance limits of our system in AWGN channel for some different source correlations (different p value) are summarized in Table I, for both *Case 1* and *Case 2*. It should be noted here that the limits for $p = 0.1, 0.05$ and 0 in *Case 1* are the same (-6.84 dB). This is because the limit is dominated by the source-destination links for $p \leq 0.1$, as shown in Fig. 7. Similar phenomena can be observed in *Case 2*, and hence in this case the limits for $p = 0.2, 0.1, 0.05$ and 0 are the same. The performance gains over "NC" and "SC", as well as the gaps to the theoretical limits with our proposed technique in both *Case 1* and *Case 2* are also summarized in Table I, at BER $= 10^{-4}$. Note that the gaps between theoretical limit and our proposed JSCN technique are roughly $1 - 2$ dB. This is because we are not using very close-limit achieving codes for per-link transmission in this paper. As shown in [24], [25], however, proper tuning of the doping rates Q_1, Q_2 and Q_r may results in even smaller gap to the limit.

C. FER Performance Evaluation in Rayleigh Fading Channels

In this subsection, the numerical results of the theoretical outage probability calculation and the FER performance of the proposed JSCN technique obtained through simulations are presented. The frame length is set at 2000 bits, and 100000 different frames were transmitted from each source node. As a reference, we provide the FER performance curves of both "NC" and "SC". The theoretical outage curve of the transmission of two uncorrelated sources to the same destination using two independent (orthogonal) time slots,[4] of which the decay corresponds to no-diversity, are also provided.

Fig. 11 demonstrates the theoretical outage curves and the FER performance of the proposed system in *Case 1*, with different source correlations. It is found that, as the source correlation becomes stronger, the theoretical outage probability decreases, since the source correlation can be exploited at the destination. Similarly, we can observe FER performance improvement by using the proposed JSCN technique as the
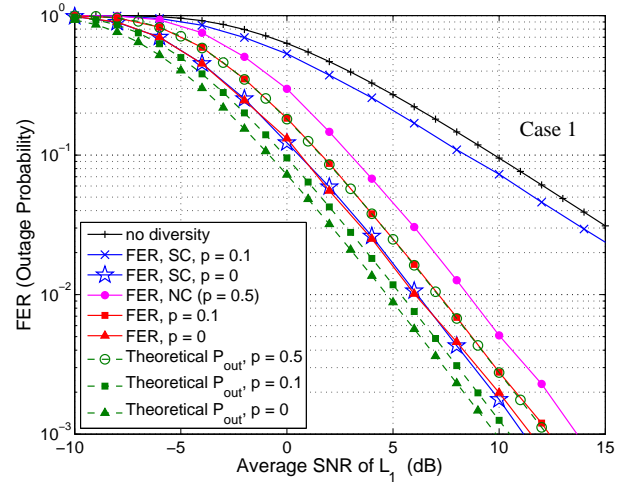
[4]There is no joint decoding at the destination. The outage event is defined as either $\mathbf{u}_1$ or $\mathbf{u}_2$ can not be decoded correctly at the destination.

Fig. 11. FER performance of the proposed JSCN technique for MARC with correlated sources in *Case 1*, with respect to the average SNR of L_1. Different source correlation are considered.

source correlation increases. Also, FER performance improvement can be observed with the proposed JSCN technique over "NC" and "SC". However, if the two sources are fully correlated ($p = 0$), the FER performance of the proposed JSCN technique and "SC" are the same. This is because of the same reason as presented in Section VI-B. For the given p values, there are around $1 - 2$ dB gaps between the FER curves obtained through simulations and the theoretical outage curves. This is because the channel codes used for the three links L_1, L_2 and L_r can not achieve very close limit performance, as indicated in Section VI-B.

The theoretical outage curves and the FER performance of the proposed system in *Case 2* are illustrated in Fig. 12. The FER and theoretical outage curves exhibit the same decay, equivalent to the *2nd* order diversity. The gaps between the FER simulation results and their corresponding theoretical outage curves are around $1 - 2$ dB. Note that if $p = 0$, the theoretical outage curve in *Case 2* is the same as that obtained in *Case 1*, which is consistent with the mathematical proof
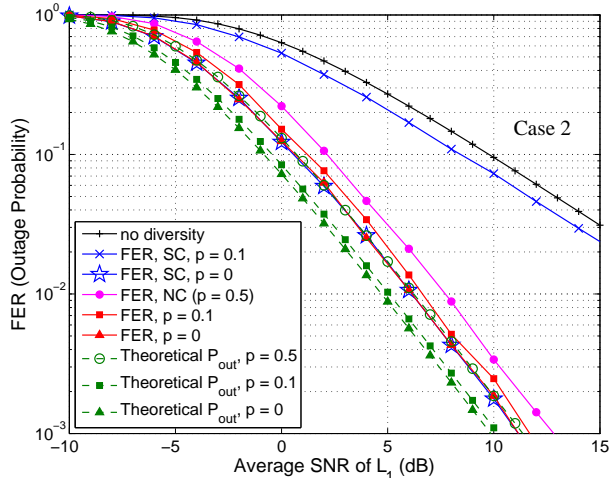
Fig. 12. FER performance of the proposed JSCN technique for MARC with correlated sources in *Case 2*, with respect to the average SNR of L_1. Different source correlation are considered.

presented in Section V-D. Furthermore, the FER curve for $p = 0$ in *Case 2* is almost the same as that obtained in *Case 1*, which also agrees with the results shown in Section VI-B.

The outage probability analysis of two correlated sources transmission without network coding in block Rayleigh fading channels is presented in [15], where it is shown that the 2*nd* order diversity can be achieved only if the two sources are correlated, and the decay asymptotically converges into no-diversity if the two sources are not fully correlated. It can be seen from Figs. 11 and 12 that the FER performance of "SC" is consistent with the results presented in [15]. However, It can also be seen from these two figures that the 2*nd* order diversity can be always achieved with the proposed JSCN technique, regardless of the p value.

It can also be observed from Figs. 11 and 12 that, as the quality of the L_r is improved (Δ increases), the theoretical outage probabilities with $p \in (0, 0.5]$ converge into the theoretical outage probabilities with $p = 0$, which is consistent with the asymptotic tendency analysis provided in Section V-D. It is expected that if the quality of L_r is good enough, the difference in theoretical outage probabilities due to different p values becomes very minor. Similar tendency can be observed in the FER performance curves obtained through simulations.

VII. CONCLUSIONS

The problem of transmitting correlated sources over orthogonal MARC has been intensively investigated in this paper, where results of theoretical analyses were presented. In order to fully exploit the source correlation while still exploiting the benefit of XOR network coding, an iterative JSCN decoding technique, which involves modified versions of the boxplus operation, was proposed for extrinsic information exchange at the destination. Furthermore, the achievable compression rate region has been studied according to the theorem for source coding with side information. It is found that the compression rate region has a three-dimensional structure, which is specified by the space surrounded by the polyhedron.

The theoretical limits for the BER performance and the outage probability of our system in AWGN channels and Rayleigh fading channels, respectively, have been calculated based on the achievable compression rate region. The asymptotic property analysis shows that, the outage probability is only determined by the quality of source-destination links if the two sources are fully correlated. Moreover, if the two sources are not fully correlated, the outage probability asymptotically converges into that obtained by assuming the two sources are fully correlated, as the average SNR of the relay-destination link increases.

A series of simulations based on some practical channel codes was conducted to verify the effectiveness of the proposed JSCN decoding technique and the results obtained from theoretical analyses. In the simulations, the two source nodes are located at the same distance to the destination node. Two different cases about the relay location are considered in this paper; in *Case 1* the relay has the same distance to the destination node as the source nodes, and in *Case 2* the relay is located closer to the destination node. The BER and FER performance results show that proposed JSCN technique achieves considerable gains over conventional MARC where the source correlation knowledge is not exploited. However, since the quality of the relay-destination link in *Case 2* is better than that in *Case 1*, the gains in *Case 2* is less than that achieved in *Case 1*. It is also found that the 2*nd* order diversity can always be achieved, regardless of the strength of the source correlation. The simulation results and the theoretical limit analysis are consistent with each other. Note that the results of the theoretical analyses include the average SNR Γ_i, and the spectrum efficiency R_{ci} representing the rate of channel coding and the modulation format for each link, only as parameters. Hence, those results can also be applied to the cases with asymmetric source-destination links and/or with higher order modulations, where it only impacts on the parallel shift of the outage curves.

Note further that this paper assumed perfect source-relay links. It is obvious, however, that the performance of the system deteriorate in the case source-relay links are also suffering from fading variations. The outage probability in the case source-relay link is also suffering from fading variations has been analyzed by [26], however, it is only for a very simple one-way relay. We believe that it is straightforward to extend the results of [26] to the case this paper has assumed. More detailed analysis is left as a future study. Furthermore, in the case of more than two users, the joint iterative decoding technique shown in [27] can be applied. In fact, the results shown in [27] indicates that the joint iterative decoding process among the users helps improve the overall performance. Similar results are expected. This is also left as a future study.

APPENDIX A
DERIVATION OF EQUATION (13)

As described in Section. II, the appearance probabilities of $\mathbf{u}_1$ and $\mathbf{u}_2$ are equiprobable, i.e., $\Pr(u_1^k) = \Pr(u_2^k) = 0.5$, we have $H(\mathbf{u}_1) = H(\mathbf{u}_2) = 1$. Furthermore, $\mathbf{u}_1$ and $\mathbf{u}_2$ are

correlated and the correlation is modeled as bit-flipping with probability p, which leads to

$$H(\mathbf{u}_1) = H(\mathbf{u}_2) = 1, \tag{32}$$

$$H(\mathbf{u}_1|\mathbf{u}_2) = H(\mathbf{u}_2|\mathbf{u}_1) = H_b(p) \tag{33}$$

$$H(\mathbf{u}_1, \mathbf{u}_2) = 1 + H_b(p). \tag{34}$$

The information sent from the relay node is $\mathbf{u}_r = \mathbf{u}_1 \oplus \mathbf{u}_2$, hence $\Pr(\mathbf{u}_r = 1) = 1 - \Pr(\mathbf{u}_r = 0) = p$. The estimate of $\mathbf{u}_r$ obtained at the destination node after decoding, $\hat{\mathbf{u}}_r$, is a bit-flipped version of $\mathbf{u}_r$ with probability α, and therefore $\Pr(\hat{\mathbf{u}}_r = 1) = 1 - \Pr(\hat{\mathbf{u}}_r) = \alpha + p - 2\alpha p$.

The mutual information between $\mathbf{u}_r$ and $\hat{\mathbf{u}}_r$ can be expressed as

$$\begin{aligned} I(\mathbf{u}_r; \hat{\mathbf{u}}_r) &= H(\hat{\mathbf{u}}_r) - H(\hat{\mathbf{u}}_r|\mathbf{u}_r) \\ &= H_b(\alpha + p - 2\alpha p) - H_b(\alpha). \end{aligned} \tag{35}$$

According to the chain rule for entropy, the joint entropy of $\mathbf{u}_1$, $\mathbf{u}_2$, $\mathbf{u}_r$ and $\hat{\mathbf{u}}_r$ can be expressed as

$$\begin{aligned} H(\mathbf{u}_1, \mathbf{u}_2, \mathbf{u}_r, \hat{\mathbf{u}}_r) = H(\mathbf{u}_1) + H(\mathbf{u}_2|\mathbf{u}_1) + H(\mathbf{u}_r|\mathbf{u}_1, \mathbf{u}_2) \\ + H(\hat{\mathbf{u}}_r|\mathbf{u}_1, \mathbf{u}_2, \mathbf{u}_r), \end{aligned} \tag{36}$$

where $H(\mathbf{u}_r|\mathbf{u}_1, \mathbf{u}_2) = 0$, and $H(\hat{\mathbf{u}}_r|\mathbf{u}_1, \mathbf{u}_2, \mathbf{u}_r) = H(\hat{\mathbf{u}}_r|\mathbf{u}_r)$. And $H(\mathbf{u}_1, \mathbf{u}_2, \mathbf{u}_r, \hat{\mathbf{u}}_r)$ can also be expressed as

$$\begin{aligned} H(\mathbf{u}_1, \mathbf{u}_2, \mathbf{u}_r, \hat{\mathbf{u}}_r) = H(\hat{\mathbf{u}}_r) + H(\mathbf{u}_1, \mathbf{u}_2|\hat{\mathbf{u}}_r) \\ + H(\mathbf{u}_r|\mathbf{u}_1, \mathbf{u}_2, \hat{\mathbf{u}}_r), \end{aligned} \tag{37}$$

where $H(\mathbf{u}_r|\mathbf{u}_1, \mathbf{u}_2, \hat{\mathbf{u}}_r) = 0$.

By combining (36) and (37), we can get

$$\begin{aligned} H(\mathbf{u}_1, \mathbf{u}_2|\hat{\mathbf{u}}_r) &= H(\mathbf{u}_1) + H(\mathbf{u}_2|\mathbf{u}_1) - [H(\hat{\mathbf{u}}_r) - H(\hat{\mathbf{u}}_r|\mathbf{u}_r)] \\ &= 1 + H_b(p) - I(\mathbf{u}_r; \hat{\mathbf{u}}_r). \end{aligned} \tag{38}$$

$H(\mathbf{u}_1, \mathbf{u}_2|\hat{\mathbf{u}}_r)$ can be further expressed as

$$\begin{aligned} H(\mathbf{u}_1, \mathbf{u}_2|\hat{\mathbf{u}}_r) &= H(\mathbf{u}_1|\hat{\mathbf{u}}_r) + H(\mathbf{u}_2|\mathbf{u}_1, \hat{\mathbf{u}}_r) \\ &= H(\mathbf{u}_2|\hat{\mathbf{u}}_r) + H(\mathbf{u}_1|\mathbf{u}_2, \hat{\mathbf{u}}_r). \end{aligned} \tag{39}$$

Given the fact that both $\mathbf{u}_1$ and $\mathbf{u}_2$ are independent of $\hat{\mathbf{u}}_r$ and $H(\mathbf{u}_1|\hat{\mathbf{u}}_r) = H(\mathbf{u}_2|\hat{\mathbf{u}}_r) = 1$, we have

$$H(\mathbf{u}_1|\mathbf{u}_2, \hat{\mathbf{u}}_r) = H(\mathbf{u}_2|\mathbf{u}_1, \hat{\mathbf{u}}_r) = H_b(p) - I(\mathbf{u}_r; \hat{\mathbf{u}}_r). \tag{40}$$

REFERENCES

[1] I. F. Akyildiz, W. Su, Y. Sankarasubramaniam, and E. Cayirci, "A survey on sensor networks," *IEEE Commun. Mag.*, vol. 40, no. 8, pp. 102–114, Aug. 2002.

[2] T. Arampatzis, J. Lygeros, and S. Manesis, "A survey of applications of wireless sensors and wireless sensor networks," in *Proc. 2005 IEEE Int. Symp. Intelligent Control*, Limassol, Cyprus, 27-29 June 2005, pp. 719–724.

[3] T. Ho, M. Medard, M. Effros, and R. Koetter, "Network coding for correlated sources," in *Proc. 38th Annu. Conf. Inform. Sci. and Syst.*, Princetion, NJ, Mar. 2004.

[4] J. Barros and S. D. Servetto, "Network information flow with correlated sources," *IEEE Trans. Inf. Theory*, vol. 52, no. 1, pp. 155–170, Jan. 2006.

[5] S. Gao, "Joint distributed source and network coding for correlated information multicasting," in *Proc. 6th Int. ICST Conf. Commun. and Networking in China (CHINACOM)*, Harbin, China, 17-19 Aug. 2011, pp. 698–702.

[6] R. Ahlswede, N. Cai, S.-Y. R. Li, and R. W. Yeung, "Network information flow," *IEEE Trans. Inf. Theory*, vol. 46, no. 4, pp. 1204–1216, July 2000.

[7] Z. Xiong, A. D. Liveris, and S. Cheng, "Distributed source coding for sensor networks," *IEEE Signal Process. Mag.*, vol. 21, no. 5, pp. 80–94, Sept. 2004.

[8] R. Joda and F. Lahouti, "Network code design for orthogonal two-hop network with broadcasting relay: A joint source-channel-network coding approach," *IEEE Trans. Commun.*, vol. 60, no. 1, pp. 132–142, Jan. 2012.

[9] T. S. Han, "Slepian-Wolf-Cover theorem for networks of channels," *Inform. and Control*, vol. 47, no. 1, pp. 67–83, Oct. 1980.

[10] J. Del Ser, P. M. Crespo, B. H. Khalaj, and J. Gutierrez-Gutierrez, "On combining distributed joint source-channel-network coding and turbo equalization in multiple access relay networks," in *Proc. 3rd IEEE Int. Conf. Wireless and Mobile Computing, Networking and Commun. (WiMob 2007)*, White Plains, NY, 8-10 Oct. 2007.

[11] Y. Wu, V. Stankovic, Z. Xiong, and S.-Y. Kung, "On practical design for joint distributed source and network coding," *IEEE Trans. Inf. Theory*, vol. 55, no. 4, pp. 1709–1720, Apr. 2009.

[12] F. P. S. Luus and B. T. Maharaj, "Joint source-channel-network coding for bidirectional wireless relays," in *Proc. IEEE Int. Conf. Acoust. Speech and Signal Process. (ICASSP)*, Prague, Czech Republic, 22-27 May 2011, pp. 3156–3159.

[13] X. Zhou, A. O. Lim, K. Anwar, and T. Matsumoto, "Distributed joint source-channel-network coding exploiting source correlation for multiple access relay channel," in *Proc. 19th European Wireless Conf.*, Guildford, UK, 16-18 April 2013, pp. 1–6.

[14] S. Katti, H. Rahul, W. Hu, D. Katabi, M. Medard, and J. Crowcroft, "XORs in the air: Practical wireless network coding," *IEEE/ACM Trans. Netw.*, vol. 16, no. 3, pp. 497–510, June 2008.

[15] M. Cheng, K. Anwar, and T. Matsumoto, "Outage probability of a relay strategy allowing intra-link errors utilizing Slepian-Wolf theorem," *EURASIP J. on Advances in Signal Process.*, vol. 2013:34, 2013.

[16] T. M. Cover and J. A. Thomas, *Elements of Information theory 2nd Edition*. USA: John Wiley & Sons, Inc., 2006.

[17] A. Gamal and Y. Kim, *Network Information Theory*. Cambridge Univ. Press, 2011.

[18] O. Iscan and C. Hausl, "Iterative network and channel decoding for the relay channel with multiple sources," in *Proc. IEEE 74th Veh. Technology Conf. (VTC Fall)*, San Francisco, CA, 5-8 Sept. 2011, pp. 1–5.

[19] P.-S. Lu, V. Tervo, K. Anwar, and T. Matsumoto, "Low-complexity strategies for multiple access relaying," in *Proc. IEEE 73rd Veh. Technology Conf. (VTC Spring)*, Budapest, Hungary, 15-18 May 2011, pp. 1–6.

[20] G. Zeitler, G. Bauch, and J. Widmer, "Quantize-and-forward schemes for the orthogonal multiple-access relay channel," *IEEE Trans. Commun.*, vol. 60, no. 4, pp. 1148–1158, Apr. 2012.

[21] S. ten Brink, "Convergence behavior of iteratively decoded parallel concatenated codes," *IEEE Trans. Commun.*, vol. 49, no. 10, pp. 1727–1737, Oct. 2001.

[22] J. Hagenauer, E. Offer, and L. Papke, "Iterative decoding of binary block and convolutional codes," *IEEE Trans. Inf. Theory*, vol. 42, no. 2, pp. 429–445, Mar. 1996.

[23] J. Garcia-Frias and Y. Zhao, "Near-shannon/slepian-wolf performance for unknown correlated sources over AWGN channels," *IEEE Trans. Commun.*, vol. 53, no. 4, pp. 555–559, Apr. 2005.

[24] K. Anwar and T. Matsumoto, "Accumulator-assisted distributed Turbo codes for relay system exploiting source-relay correlations," *IEEE Commun. Lett.*, vol. 16, no. 7, pp. 1114–1117, July 2012.

[25] A. Irawan, K. Anwar, and T. Matsumoto, "Combining-after-decoding turbo hybrid ARQ by utilizing doped-accumulator," *IEEE Commun. Lett.*, vol. 17, no. 6, pp. 1212–1215, June 2013.

[26] X. Zhou, M. Cheng, X. He, and T. Matsumoto, "Outage probability of decode-and-forward relaying system allowing intra-link errors in rayleigh fading channels," in *2014 IEEE Int. Conf. on Commun. (ICC 2014)*, submitted.

[27] P.-S. Lu, X. Zhou, K. Anwar, and T. Matsumoto, "Joint adaptive network-channel coding for energy-efficient multiple access relaying," *IEEE Trans. Veh. Technol.*, to be published.
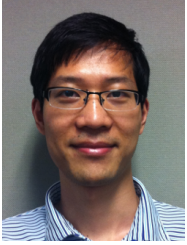
Xiaobo Zhou (S'11−M'13) recieved the B.Sc. in Electronic Information Science and Technology from University of Science and Technology of China (USTC), Hefei, China, in 2007, the M.E. in Computer Application Technology from Graduate University of Chinese Academy of Science (GU-CAS), Beijing, China, in 2010, and the Ph.D. degree from School of Information Science, Japan Advanced Institute of Science and Technology (JAIST), Ishikawa, Japan, in 2013. Since October 2013, he is with the School of Information Science, JAIST as a researcher. His research interests include coding techniques, joint source-channel coding, cooperative wireless communications and network information theory.

Pen-Shun Lu (S'09) received the B.S. degree in electrical engineering from National Sun Yat-Sen University (NSYSU), Taiwan, in 2003 and the M.Sc in wireless communications from the University of Southampton, UK, in 2007. Currently he is pursuing the PhD degrees in University of Oulu, Finland and Japan Advanced Institute of Science and Technology (JAIST), Japan. His current research interests include joint source and channel coding, distributed coding, iterative detection and cooperative communications.

Khoirul Anwar (S'03−M'08) graduated (*cum laude*) from the department of Electrical Engineering (Telecommunications), Institut Teknologi Bandung (ITB), Bandung, Indonesia in 2000. He received Master and Doctor Degrees from Graduate School of Information Science, Nara Institute of Science and Technology (NAIST) in 2005 and 2008, respectively. Since then, he has been appointed as an assistant professor in NAIST. He received best student paper award from the IEEE Radio and Wireless Symposium 2006 (RWS '06), California-USA, Best Paper of Indonesian Student Association (ISA '07), Kyoto, Japan in 2007, and Award for Innovation, Congress of Indonesian Diaspora (CID), Los Angels, USA, July 2012. Since September 2008, he is with the School of Information Science, Japan Advanced Institute of Science and Technology (JAIST) as an assistant professor. His research interests are network information theory, error control coding, iterative decoding and signal processing for wireless communications. Dr. Anwar is a member of IEEE, information theory society, communication society and IEICE Japan.

Tad Matsumoto (S'84−SM'95−F'10) received his B.S., M.S., and Ph.D. degrees from Keio University, Yokohama, Japan, in 1978, 1980, and 1991, respectively, all in electrical engineering. He joined Nippon Telegraph and Telephone Corporation (NTT) in April 1980. Since he engaged in NTT, he was involved in a lot of research and development projects, all for mobile wireless communications systems. In July 1992, he transferred to NTT DoCoMo, where he researched Code-Division Multiple-Access techniques for Mobile Communication Systems. In April 1994, he transferred to NTT America, where he served as a Senior Technical Advisor of a joint project between NTT and NEXTEL Communications. In March 1996, he returned to NTT DoCoMo, where he served as a Head of the Radio Signal Processing Laboratory. In March 2002, he moved to University of Oulu, Finland, where he served as a Professor at Centre for Wireless Communications. In 2006, he served as a Visiting Professor at Ilmenau University of Technology, Ilmenau, Germany, funded by the German MERCATOR Visiting Professorship Program. In April 2007, he returned to Japan and since then he has been serving as a Professor at Japan Advanced Institute of Science and Technology (JAIST), while also keeping a part-time position at University of Oulu. Prof. Matsumoto has been appointed as a Finland Distinguished Professor for a period from January 2008 through December 2012, funded by the Finnish National Technology Agency (Tekes) and Finnish Academy, under which he preserves the rights to participate in and apply to European and Finnish national projects. Prof. Matsumoto is a recipient of IEEE VTS Outstanding Service Award (2001), Nokia Foundation Visiting Fellow Scholarship Award (2002), IEEE Japan Council Award for Distinguished Service to the Society (2006), IEEE Vehicular Technology Society James R. Evans Avant Garde Award (2006), and Thuringen State Research Award for Advanced Applied Science (2006), 2007 Best Paper Award of Institute of Electrical, Communication, and Information Engineers (IEICE) of Japan (2008), Telecom System Technology Award by the Telecommunications Advancement Foundation (2009), IEEE Communication Letters Exemplifying Reviewer Award (2011), UK Royal Academy of Engineering Distinguished Visiting Fellow Award (2012) and Nikkei Electronic Wireless Japan Awards (2013). He is serving as an IEEE Vehicular Technology Distinguished Lecturer since July 2011. He is a Fellow of IEEE and a member of IEICE.